PAMELA: A Satellite Experiment for Antiparticles Measurement in Cosmic Rays

Massimo Bongi, O. Adriani, M. Ambriola, A. Bakaldin, G. C. Barbarino, A. Basili, G. Bazilevskaja, R. Bellotti, R. Bencardino, M. Boezio, E. A. Bogomolov, L. Bonechi, L. Bongiorno, V. Bonvicini, M. Boscherini, F. S. Cafagna, D. Campana, P. Carlson, M. Casolino, G. Castellini, M. Circella, C. N. De Marzo, M. P. De Pascale, G. Furano, A. M. Galper, N. Giglietto, A. Grigorjeva, S. V. Koldashov, M. G. Korotkov, S. Y. Krut'kov, J. Lund, J. Lundquist, A. Menicucci, W. Menn, V. V. Mikhailov, M. Minori, N. Mirizzi, J. W. Mitchell, E. Mocchiutti, A. Morselli, R. Mukhametshin, S. Orsi, G. Osteria, P. Papini, M. Pearce, P. Picozza, M. Ricci, S. B. Ricciarini, M. Romita, G. Rossi, S. Russo, P. Schiavon, M. Simon, R. Sparvoli, P. Spillantini, P. Spinelli, S. J. Stochaj, Y. Stozhkov, S. Straulino, R. E. Streitmatter, F. Taccetti, A. Vacchi, E. Vannuccini, G. I. Vasilyev, S. A. Voronov, R. Wischnewski, Y. Yurkin, G. Zampa, and N. Zampa

***Abstract*—PAMELA is a satellite-borne experiment that will study the antiproton and positron fluxes in cosmic rays in a wide range of energy (from 80 MeV up to 190 GeV for antiprotons and from 50 MeV up to 270 GeV for positrons) and with high statistics, and that will measure the antihelium/helium ratio with a sensitivity of the order of 10^{-8}. The detector will fly on-board a polar orbiting Resurs DK1 satellite, which will be launched into space by a Soyuz rocket in 2004 from Baikonur cosmodrome in Kazakhstan, for a 3-year-long mission. Particle identification and energy measurements are performed in the PAMELA apparatus using the following subdetectors: a magnetic spectrometer made up of a permanent magnet equipped with double-sided microstrip silicon detectors, an electromagnetic imaging calorimeter composed of layers of tungsten absorber and silicon detectors planes, a transition radiation detector made of straw tubes interleaved with carbon fiber radiators, a plastic scintillator time-of-flight and trigger system, a set of anticounter plastic scintillator detectors, and a neutron detector. The features of the detectors and the main results obtained in beam test sessions are presented.**

***Index Terms*—Antimatter, cosmic rays, satellite experiment.**

Manuscript received November 21, 2003; revised March 22, 2004.

M. Bongi is with INFN–Sezione di Firenze, 1-50019 Sesto Fiorentino (FI), Italy (e-mail: bongi@fi.infn.it).

O. Adriani, L. Bonechi, P. Papini, S. B. Ricciarini, P. Spillantini, S. Straulino, F. Taccetti, and E. Vannuccini are with Università di Firenze and INFN, 1-50019 Sesto Fiorentino, Italy.

M. Ambriola, R. Bellotti, F. S. Cafagna, M. Circella, C. N. De Marzo, N. Giglietto, N. Mirizzi, M. Romita, and P. Spinelli are with Università di Bari and INFN, Bari 70426, Italy.

A. Bakaldin, A. M. Galper, S. V. Koldashov, M. G. Korotkov, V. V. Mikhailov, S. A. Voronov, and Y. Yurkin are with Moscow Engineering and Physics Institute, Moscow 115409, Russia.

G. C. Barbarino, D. Campana, G. Osteria, G. Rossi, and S. Russo are with Dipartamento di Scienze Fisiche, Università "Federico II" and INFN, Napoli 80126, Italy.

A. Basili, R. Bencardino, L. Bongiorno, M. Casolino, M. P. De Pascale, G. Furano, A. Menicucci, M. Minori, A. Morselli, P. Picozza, R. Sparvoli, and R. Wischnewski are with Università "Tor Vergata" and INFN, Roma-Tor Vergata 00133, Italy.

G. Bazilevskaja, A. Grigorjeva, R. Mukhametshin, and Y. Stozhkov are with Lebedev Physical Institute, Moscow 119 991, Russia.

M. Boezio, V. Bonvicini, P. Schiavon, A. Vacchi, G. Zampa, and N. Zampa are with Università di Trieste and INFN, Trieste 34127, Italy.

E. A. Bogomolov, G. I. Vasilyev, and S. Y. Krut'kov are with Ioffe Physico-Technical Institute, St. Petersburg 194 021, Russia.

M. Boscherini, W. Menn, and M. Simon are with Universitaet-GH Siegen, FB Physik, Siegen 57068, Germany.

P. Carlson, J. Lund, S. Orsi, and M. Pearce are with the Royal Institute of Technology, Stockholm 10691, Sweden.

G. Castellini is with Istituto di Fisica Applicata "N. Carrara," CNR, Firenze 50127, Italy.

J. W. Mitchell and R. E. Streitmatter are with NASA Goddard Space Flight Center, Greenbelt, MD 20771 USA.

E. Mocchiutti was with Università di Trieste and INFN, Trieste, Italy. He is now with the Royal Institute of Technology, Stockholm 10691, Sweden.

J. Lundquist was with the Royal Institute of Technology, Stockholm, Sweden. He is now with Università di Trieste and INFN, Trieste 34127, Italy

M. Ricci is with Laboratori Nazionali INFN, Frascati 00044, Italy.

S. J. Stochaj is with Particle Astrophysics Laboratory, NMSU, Las Cruces, NM 88003-8001 USA.

Digital Object Identifier 10.1109/TNS.2004.829504

I. Introduction

PAMELA (a Payload for Antimatter Matter Exploration and Light-nuclei Astrophysics) [1] is a satellite-borne experiment that has been designed to study charged particles in cosmic rays. The detector will be mounted in a pressurized vessel attached to a Russian Earth-observation satellite, the Resurs DK1, which will be launched into space by a Soyuz rocket in 2004 from Baikonur cosmodrome in Kazakhstan. The orbit will be elliptical and semi-polar, with an inclination of 70.4° and an altitude varying between 350 and 600 km.

During its at least 3-year-long mission, PAMELA will measure with high precision the energy spectrum and the composition of the cosmic radiation, in particular looking for its antimatter component. It will extend the currently explored region of the antiprotons and positrons spectrum both toward higher and lower energies. The characteristics of the orbit will grant PAMELA sensitivity to the low energy region because of the lower Earth's geomagnetic cutoff near the poles.

II. Scientific Objectives

The primary objective of the PAMELA experiment is to detect and identify antiprotons and positrons in cosmic radiation, measuring their spectrum in a wide energy range (80 MeV–190 GeV for antiprotons, 50 MeV–270 GeV for positrons) with statistics never reached before ($\sim 10^4$ and $\sim 10^5$ particles/year, respectively).

Almost all data available so far about cosmic antiprotons and positrons have been obtained using detectors in balloon-borne

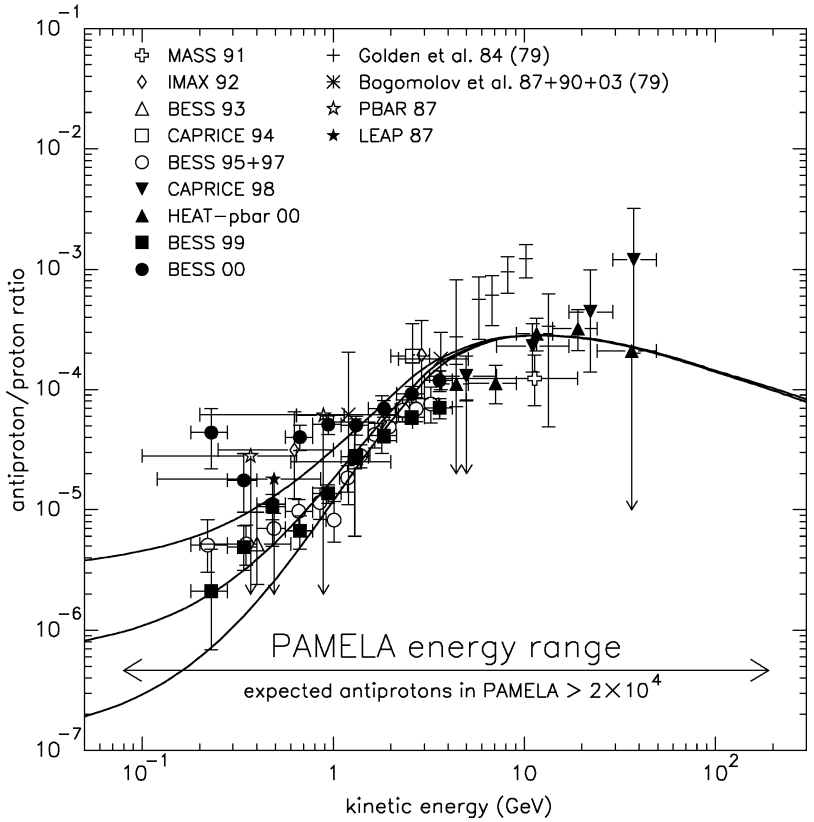

Fig. 1. Antiproton-to-proton ratio at the top of the atmosphere. PAMELA expected energy range is shown. References are: Golden *et al.* [7], [8], Bogomolov *et al.* [9] and references therein, LEAP 87 [10], PBAR 87 [11], MASS 91 [12], IMAX 92 [13], BESS 93 [14], CAPRICE 94 [15], BESS 95+97 [16], CAPRICE 98 [17], HEAT-pbar 00 [18], and BESS 99 and 00 [19]. Lines represent theoretical calculations based on a purely secondary production of antiprotons [20].

experiments. The short data-taking time (approximately 24 h) and the presence of a residual amount of the Earth's atmosphere above the detecting apparatus at altitudes that a balloon can reach (from $\sim$ 10 g/cm^2 around 30 km, to $\sim$ 3 g/cm^2 around 40 km) are the main limits of such kind of measurements.

Figs. 1 and 2 summarize the current situation in antiproton and positron measurements in cosmic rays. A satellite-borne experiment such as PAMELA will be able to do more precise measurements and cover a wider range of energy, thanks to the lack of atmospheric overburden and the longer data-taking time. This will allow us to discriminate among competing models of antimatter production in our galaxy or to identify primary sources of cosmic antimatter.

The PAMELA experiment will also look for light antinuclei in cosmic rays, measuring the $\overline{\mathrm{He}}$/He ratio with a sensitivity $\sim 10^{-8}$, and it will study ordinary matter cosmic rays as well, detecting protons, electron, and light nuclei up to $\mathrm{Z} = 6$.

Table I summarizes the expected particle samples after three years of operation of the detector.

TABLE I
EXPECTED PARTICLE SAMPLES AFTER A 3-YEAR PAMELA MISSION

Particle	Number (3 years)	Energy Range
Protons	3×10^8	80 MeV - 700 GeV
Antiprotons	$>3 \times 10^4$	80 MeV - 190 GeV
Electrons	6×10^6	50 MeV - 2 TeV
Positrons	$>3 \times 10^5$	50 MeV - 270 GeV
He	4×10^7	80 MeV/n - 700 GeV/n
Be	4×10^4	80 MeV/n - 700 GeV/n
C	5×10^5	80 MeV/n - 700 GeV/n
$\overline{\mathrm{He}}$/He limit at 90% C.L.	7×10^{-8}	80 MeV/n - 30 GeV/n

III. PAMELA SUBDETECTORS

PAMELA (see Fig. 3) is built around a permanent magnetic spectrometer equipped with a silicon tracking system, which is used to measure the momentum, the sign, and the absolute charge of particles passing through the cavity of the magnet. An anticounter system (AC) surrounds the magnet and allows rejection of particles which do not pass cleanly through the acceptance window of the tracker. An electromagnetic calorimeter measures the energy of electrons and positrons and it is used for particle identification through the topological discrimination of the shower. In this task it is complemented at energies below 1 GeV by time-of-flight (ToF) measurements made by a scintillator system, which also provides the primary experimental trigger, and at energies above 1 GeV by a transition radiation detector (TRD), which makes particle identification through threshold velocity measurements. A bottom scintillator and a neutron detector placed below the apparatus will provide additional information which will help in distinguishing electromagnetic and hadronic showers in the calorimeter.

The detector is approximately 130 cm high, its mass is about 450 kg, and the power consumption is 350 W.

In this section, a more detailed overview of each PAMELA subdetector and the main results from beam test sessions are given.

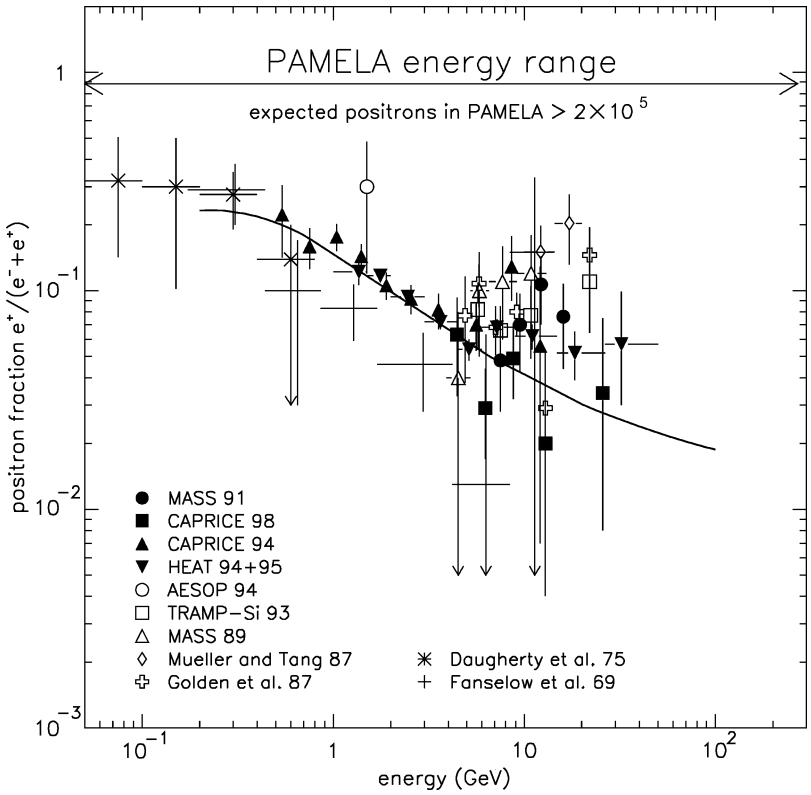

Fig. 2. Positron fraction at the top of the atmosphere. PAMELA expected energy range is shown. References are: Fanselow *et al.* [21], Daugherty *et al.* [22], Golden *et al.* [23], Mueller and Tang [24], MASS 89 [25], TRAMP-Si 93 [26], AESOP 94 [27], HEAT 94+95 [28], CAPRICE 94 [29], CAPRICE 98 [30], and MASS 91 [31]. The line represents a theoretical calculation based on a purely secondary production of positrons [32].

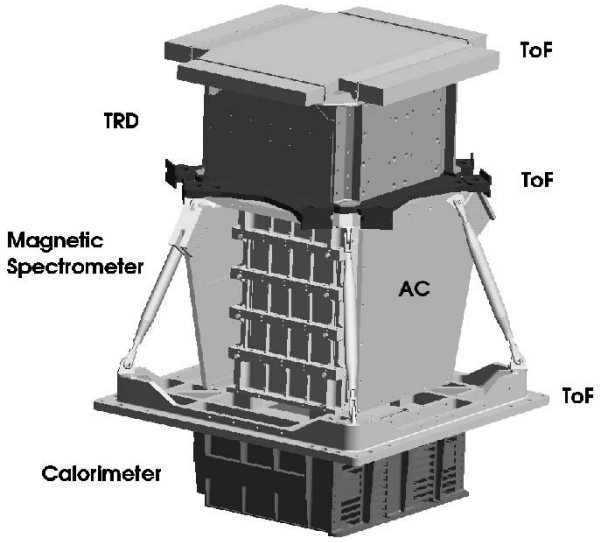

Fig. 3. Schematic view of the PAMELA detector, in which the mutual positions of the subsystems are shown.

A. Magnetic Spectrometer

The central part of PAMELA apparatus is a magnetic spectrometer [2] consisting of a permanent magnet and a silicon tracker.

The magnet is made up of five modules of a sintered Nd–Fe–B alloy with a residual magnetic induction of about 1.3 T. The tracking cavity is 445 mm tall and has a cross section of 132 mm $\times$ 162 mm, which gives 20.5 cm^{2}sr as the geometric factor of the detector. The particular magnetic configuration permits a nearly uniform magnetic field inside the spectrometer cavity of about 0.4 T.

The tracking system is composed of six detecting planes interleaved with the magnetic modules. Each plane is made up of six double-sided microstrip silicon detectors, 300 μm thick. The strip pitch is 25 μm for the junction side (which is used to measure the coordinate in the bending plane of the particles inside the magnetic cavity) and one strip out of two is connected to the readout electronics. On the ohmic side the pitch is 67 μm, strips are orthogonally implanted with respect to the previous ones, and a double metal layer is used in order to have the readout electronics on the same sensor edge for both sides. This configuration gives a total of 6144 readout channels for each of the six planes. The charge produced within silicon by ionizing particles is collected by the strips and used to reconstruct the impact points on the spectrometer's planes. In order to reduce the amount of data to be transmitted from the satellite a compression algorithm has been developed. The compression factor that has been obtained is about 95%, with no degradation of the detector response.

Data acquired in beam test sessions allowed a measure of the spatial resolution of the silicon detectors (see Fig. 4). The result that has been obtained is about 3 μm for the particle bending direction and about 11 μm for the orthogonal coordinate (Gaussian fit). The resulting maximum detectable rigidity for the spectrometer exceeds 740 GV/c.

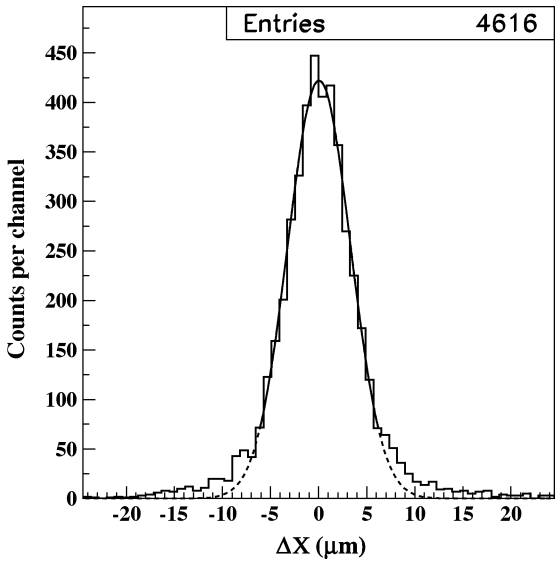

Fig. 4. Spatial resolution in the bending view for the tracker silicon detectors.

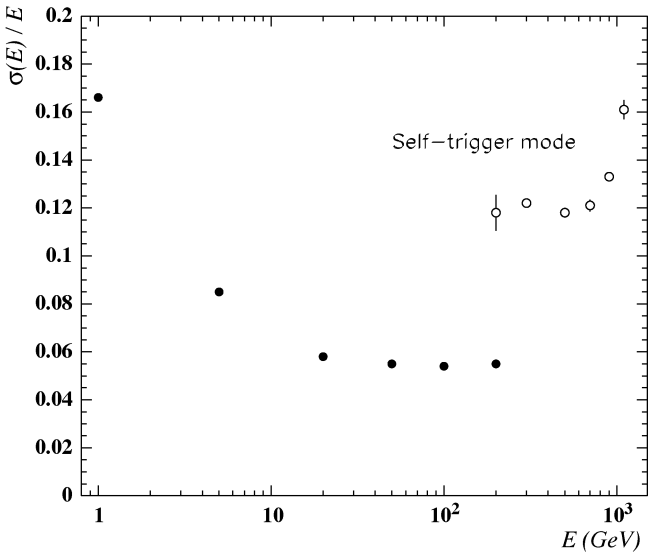

Fig. 5. Energy resolution of the electromagnetic calorimeter as a function of energy for electrons and positrons. The filled dots are for normal operation, while the open dots are for self-triggering mode.

B. Anticounter System

The anticounter system [3] consists of four lateral detectors covering the sides of the tracker and one top detector above the tracker. Each detector is made from a sheet of plastic scintillator read out by multiple compact photomultiplier tubes, equipped with a LED based system for in-flight checks.

The efficiency for detecting minimum ionizing particles has been measured using cosmic ray muons and it has been found to exceed 99.9% per detector, thus permitting us to exclude from offline analysis particles which do not pass within the geometrical acceptance of the tracking system.

C. Electromagnetic Imaging Calorimeter

The electromagnetic calorimeter [4] is made from 44 planes of single-sided silicon detectors interleaved with 22 layers of tungsten absorbers. The detecting planes are 380 μm thick and segmented in 2.4 mm strips, while the absorber layers are 2.6 mm thick. The total depth of the calorimeter is about 16.3 radiation lengths and about 0.6 interaction length.

The strips are arranged in a Si-x/W/Si-y geometry in order to allow topological reconstruction of the shower. It is thus possible to distinguish electrons and positrons from hadrons or noninteracting particles, obtaining a rejection factor of better than 10^4 between protons (antiprotons) and positrons (electrons) at 95% retaining efficiency. The achieved energy resolution in beam test sessions is about 5.5% in the range 20–200 GeV, as shown in Fig. 5.

The calorimeter can also be operated in self-trigger mode: this hardware feature allows the stand-alone detection of e^- with an increased acceptance of 470 $\mathrm{cm}^2\mathrm{sr}$ up to an energy of about 2 TeV. Fig. 5 shows that an energy resolution of about 12% has been obtained in the range 200–700 GeV: the rising of $\sigma(\mathrm{E})/\mathrm{E}$ for higher energies is due to the incomplete shower containment at these energies.

D. Time-of-Flight (ToF) System

The ToF system [5] is composed of six layers of segmented plastic scintillators arranged in three planes and read out by photomultiplier tubes. The three planes are located above the TRD, between the TRD and the spectrometer, and between the spectrometer and the calorimeter (see Fig. 3).

The ToF provides a fast signal for triggering data acquisition in the other subdetectors, determines the absolute value of the charge Z of incident particles through multiple measurements of the energy loss dE/dx in the planes, and finally measures the flight time of particles crossing its planes. Once this information is integrated with the measurement of the trajectory length done by the tracking system, the velocity of the particle can be calculated. This feature also enables the rejection of albedo particles.

An evaluation of the timing resolution of the planes has been performed comparing the impact point reconstruction done by the scintillator with the impact point obtained by an external drift chamber. Fig. 6 shows the distribution of the difference (converted to a time) between the impact point reconstructed by the ToF and the one obtained by the drift chamber, after corrections for time walk have been applied. The resulting timing resolution allows for a 3σ separation between protons (antiprotons) and positrons (electrons) up to about 1.5 GeV.

E. Transition Radiation Detector

PAMELA TRD [6] is a detector made up of 10 carbon-fiber radiator layers interleaved with 9 planes of Xe–CO_2 straw tubes working in a proportional regime at a 1400 V voltage, arranged in a truncated pyramid shape. A single straw tube is 280 mm in length and 4 mm in diameter. It is made of a copper-clad Kapton foil, 30 μm thick, with a tungsten anode wire, 25 μm in diameter, stretched up to a 60 g tension, on the inside.

Relativistic particles crossing boundaries of materials with different dielectric constants (the carbon-fiber radiator layers interfaces) will emit transition radiation in the X-ray range, which is then detected by the gas detectors. For a given momentum,

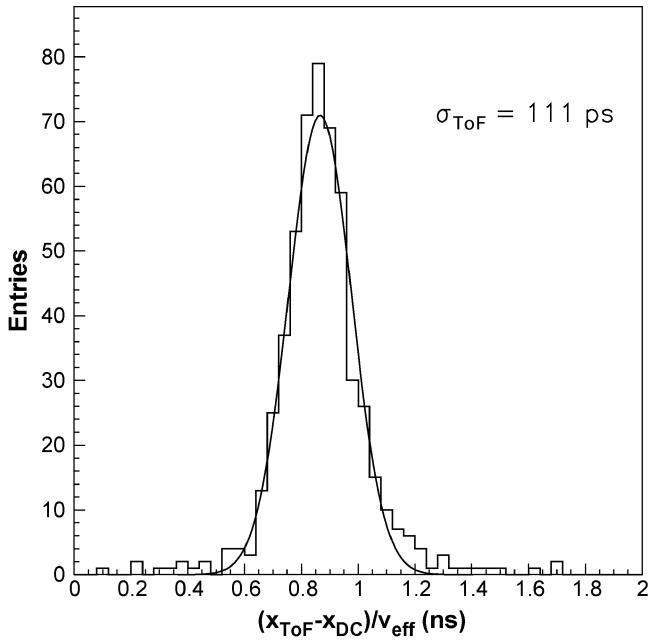

Fig. 6. Timing resolution for a ToF paddle, after correcting for time walk.

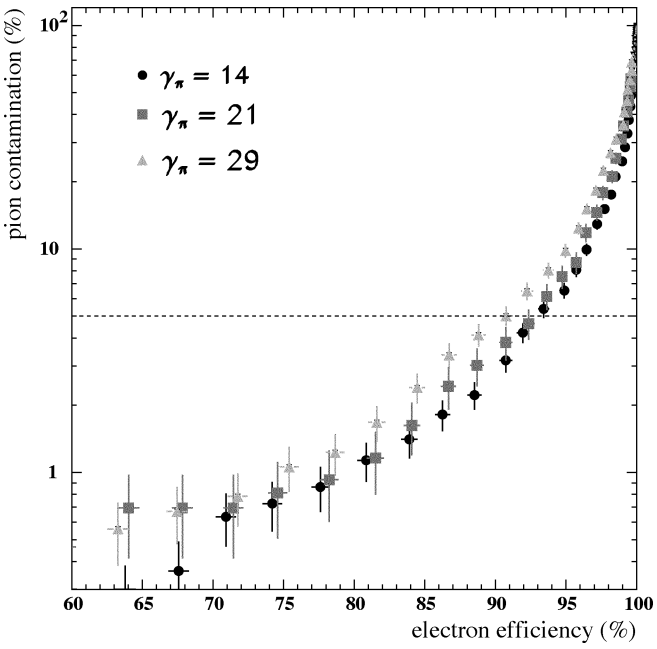

Fig. 7. Pion contamination versus electron discrimination efficiency at different Lorentz factors for the transition radiation detector.

the TRD allows a lepton–hadron separation through threshold velocity measurement. A discrimination efficiency of 90% for radiating particles with a contamination at a level of 5% from nonradiating particles has been obtained in the PAMELA range of investigation (see Fig. 7).

F. Bottom Scintillator and Neutron Detector

A plastic scintillator plane located under the calorimeter detects particles escaping from it: this bottom scintillator is used to provide an additional trigger for high energy (>100 GeV) electrons. It also triggers the neutron detector housed below it.

The purpose of this ^{3}He neutron detector is to extend the electron–proton discrimination capabilities of the PAMELA apparatus up to 10^{11}–10^{13} eV. A large neutron component will accompany high energy hadronic showers developed in the calorimeter.

IV. Conclusion

In preparation to the space mission, extensive space qualification tests on PAMELA detectors, electronics, and mechanical structures have been developed and are still in progress. During 2000 and 2001, the mass and thermal model and the engineering model of PAMELA subdetectors were qualified for space flight through vibration, thermal, irradiation test and laboratory studies. So far, all detectors have proved their capability to withstand the severe conditions of the rocket launch. Final qualification tests on the mass and thermal model of the PAMELA apparatus are ongoing at the TsSKB-Progress factory in Samara, Russia.

Furthermore, detector performances have been verified in test experiments at the PS and SPS beams at CERN. Tests performed so far show that all the detectors of the PAMELA apparatus comply with their design performance. The latest tests were carried out in September 2003 at SPS in an almost complete flight model setup.

Integration of the flight model versions of all subdetectors is underway in Rome. PAMELA will then be taken to TsSKB-Progress for integration with the Resurs DK1 satellite in early 2004. The launch is scheduled for the first half of 2004.

References

[1] M. Simon (on behalf of the PAMELA Collaboration), "Status of the PAMELA experiment on-board of the resurs DK-1 spacecraft," in *Proc. 28th Int. Cosmic Ray Conf.*, Tsukuba, Japan, 2003, OG 1.5, pp. 2117–2120.

[2] O. Adriani, L. Bonechi, M. Bongi, G. Castellini, R. D'Alessandro, and A. Gabbanini *et al.*, "The magnetic spectrometer of the PAMELA satellite experiment," *Nucl. Instrum. Meth.*, vol. A511, pp. 72–75, 2003.

[3] M. Pearce, P. Carlson, J. Lund, J. Lundquist, S. Orsi, and S. Rydstroem, "The anticounter system of the PAMELA space experiment," in *Proc. 28th Int. Cosmic Ray Conf.*, Tsukuba, Japan, 2003, OG 1.5, pp. 2125–2128.

[4] M. Boezio, V. Bonvicini, E. Mocchiutti, P. Schiavon, G. Scian, and A. Vacchi *et al.*, "A high granularity imaging calorimeter for cosmic-ray physics," *Nucl. Instrum. Meth.*, vol. A487, pp. 407–422, 2002.

[5] D. Campana, G. Barbarino, M. Boscherini, W. Fuernkranz, W. Menn, and J. Mitchell *et al.*, "The time-of-flight system of the PAMELA experiment," in *Proc. 28th Int. Cosmic Ray Conf.*, Tsukuba, Japan, 2003, OG 1.5, pp. 2141–2144.

[6] M. Ambriola, R. Bellotti, F. Cafagna, M. Circella, C. De Marzo, and N. Giglietto *et al.*, "PAMELA space mission: the transition radiation detector," in *Proc. 28th Int. Cosmic Ray Conf.*, Tsukuba, Japan, 2003, OG 1.5, pp. 2121–2124.

[7] R. L. Golden, S. Horan, B. G. Mauger, G. D. Badhwar, J. L. Lacy, and S. A. Stephens *et al.*, "Evidence for the existence of cosmic-ray antiprotons," *Phys. Rev. Lett.*, vol. 43, pp. 1196–1199, 1979.

[8] R. L. Golden, B. G. Mauger, S. Nunn, and S. Horan, "Energy dependence of the p-bar/p ratio in cosmic rays," *Astrophys. Lett.*, vol. 24, pp. 75–83, 1984.

[9] E. A. Bogomolov, G. I. Vasilyev, S. Y. Krut'kov, S. V. Stepanov, and M. S. Shulakova, "Antiprotons and deuterons in galactic cosmic rays," *Proc. Russian Acad. Sci. (Phys. Ser.)*, vol. 67, pp. 447–451, 2003.

[10] R. E. Streitmatter, J. S. Stochaj, F. J. Ormes, L. R. Golden, A. S. Stephens, and T. Bowen *et al.*, "Experimental limit on low energy antiprotons in the cosmic radiation," in *Proc. 21th Int. Cosmic Ray Conf.*, vol. 3 (OG), Adelaide, Australia, 1990, pp. 277–280.

[11] M. H. Salamon, S. McKee, J. A. Musser, G. Tarle, A. Tomasch, and C. R. Bower *et al.*, "Limits on the antiproton/proton ratio in the cosmic radiation from 100 MeV to 1580 MeV," *Astrophys. J.*, vol. 349, pp. 78–90, 1990.

[12] M. Hof, W. Menn, C. Pfeifer, M. Simon, R. L. Golden, and S. J. Stochaj *et al.*, "Measurement of cosmic-ray antiprotons from 3.7 to 19 GeV," *Astrophys. J. Lett.*, vol. 467, pp. 33–36, 1996.

[13] J. W. Mitchell, L. M. Barbier, E. R. Christian, J. F. Krizmanic, K. Krombel, and J. F. Ormes *et al.*, "Measurement of 0.25–3.2 GeV antiprotons in the cosmic radiation," *Phys. Rev. Lett.*, vol. 76, pp. 3057–3060, 1996.

[14] A. Moiseev, K. Yoshimura, I. Ueda, K. Anraku, R. Golden, and M. Imori *et al.*, "Cosmic-ray antiproton flux in the energy range from 200 to 600 MeV," *Astrophys. J.*, vol. 474, pp. 479–489, 1997.

[15] M. Boezio, P. Carlson, T. Francke, N. Weber, M. Suffert, and M. Hof *et al.*, "The cosmic ray antiproton flux between 0.62 and 3.19 GeV measured near solar minimum activity," *Astrophys. J.*, vol. 487, pp. 415–423, 1997.

[16] S. Orito, T. Maeno, H. Matsunaga, K. Abe, K. Anraku, and Y. Asaoka *et al.*, "Precision measurement of cosmic-ray antiproton spectrum," *Phys. Rev. Lett.*, vol. 84, pp. 1078–1081, 2000.

[17] M. Boezio, V. Bonvicini, P. Schiavon, A. Vacchi, N. Zampa, and D. Bergstroem *et al.*, "The cosmic-ray antiproton flux between 3 and 49 GeV," *Astrophys. J.*, vol. 561, pp. 787–799, 2001.

[18] A. S. Beach, J. J. Beatty, A. Bhattacharyya, C. Bower, S. Coutu, and M. A. Duvernois *et al.*, "Measurement of the cosmic-ray antiproton-to-proton abundance ratio between 4 and 50 GeV," *Phys. Rev. Lett.*, vol. 87, pp. 271 101/1–271 101/4, 2001.

[19] Y. Asaoka, Y. Shikaze, K. Abe, K. Anraku, M. Fujikawa, and H. Fuke *et al.*, "Measurements of cosmic-ray low-energy antiproton and proton spectra in a transient period of solar field reversal," *Phys. Rev. Lett.*, vol. 88, pp. 051 101/1–051 101/4, 2002.

[20] A. Molnar and M. Simon, "A new calculation of the interstellar secondary cosmic ray antiprotons," in *Proc. 27th Int. Cosmic Ray Conf.*, Hamburg, Germany, 2001, OG 043, pp. 1877–1879.

[21] J. L. Fanselow, R. C. Hartman, R. H. Hildebrand, and P. Meyer, "Charge composition and energy spectrum of primary cosmic-ray electrons," *Astrophys. J.*, vol. 158, pp. 771–780, 1969.

[22] J. K. Daugherty, R. C. Hartman, and P. J. Schmidt, "A measurement of cosmic-ray positron and negatron spectra between 50 and 800 MV," *Astrophys. J.*, vol. 198, pp. 493–505, 1975.

[23] R. L. Golden, B. G. Mauger, S. Horan, S. A. Stephens, R. R. Daniel, and G. D. Badhwar *et al.*, "Observation of cosmic ray positrons in the region from 5 to 50 GeV," *Astron. & Astrophys.*, vol. 188, pp. 145–154, 1987.

[24] D. Mueller and K. Tang, "Cosmic-ray positrons from 10 to 20 GeV: a balloon-borne measurement using the geomagnetic east-west asymmetry," *Astrophys. Jour.*, vol. 312, pp. 183–194, 1987.

[25] R. L. Golden, B. G. Mauger, S. Horan, S. A. Stephens, R. R. Daniel, and G. D. Badhwar *et al.*, "Observations of cosmic-ray electrons and positrons using an imaging calorimeter," *Astrophys. J.*, vol. 436, pp. 769–775, 1994.

[26] R. L. Golden, S. J. Stochaj, S. A. Stephens, F. Aversa, G. Barbiellini, and M. Boezio *et al.*, "Measurement of the positron to electron ratio in the cosmic rays above 5 GeV," *Astrophys. J. Lett.*, vol. 457, pp. 103–106, 1996.

[27] J. M. Clem, D. P. Clements, J. Esposito, P. Evenson, D. Huber, and J. L'Heureux *et al.*, "Solar modulation of cosmic electrons," *Astrophys. J.*, vol. 464, pp. 507–515, 1996.

[28] S. W. Barwick, J. J. Beatty, A. Bhattacharyya, C. R. Bower, C. J. Chaput, and S. Coutu *et al.*, "Measurements of the cosmic-ray positron fraction from 1 to 50 GeV," *Astrophys. J. Lett.*, vol. 482, pp. 191–194, 1997.

[29] M. Boezio, P. Carlson, T. Francke, N. Weber, M. Suffert, and M. Hof *et al.*, "The cosmic ray electron and positron spectra measured at 1 AU during solar minimum activity," *Astrophys. J.*, vol. 532, pp. 653–669, 2000.

[30] M. Boezio, G. Barbiellini, V. Bonvicini, P. Schiavon, A. Vacchi, and N. Zampa *et al.*, "Measurements of cosmic-ray electrons and positrons by the WiZard/CAPRICE collaboration," *Advances Space Res.*, vol. 27, pp. 669–674, 2001.

[31] C. Grimani, S. A. Stephens, F. S. Cafagna, G. Basini, R. Bellotti, and M. T. Brunetti *et al.*, "Measurement of the absolute energy spectra of cosmic-ray positrons and electrons above 7 GeV," *Astron. & Astrophys.*, vol. 392, pp. 287–294, 2002.

[32] I. V. Moskalenko and A. W. Strong, "Production and propagation of cosmic-ray positrons and electrons," *Astrophys. J.*, vol. 493, pp. 694–707, 1998.